BJP British Journal of Pharmacology

DOI:10.1111/bph.12726
www.brjpharmacol.org

RESEARCH PAPER

Revisiting CFTR inhibition: a comparative study of $CFTR_{inh}$-172 and GlyH-101 inhibitors

N Melis, M Tauc, M Cougnon, S Bendahhou, S Giuliano, I Rubera and C Duranton

University of Nice-Sophia Antipolis, LP2M CNRS-UMR7370, Faculté de médecine, Nice, France

Correspondence
Duranton Christophe, University of Nice-Sophia Antipolis, LP2M CNRS-UMR7370, faculté de medecine, 06108 Nice, France.
Email: duranton@unice.fr

Received
5 November 2013
Revised
4 April 2014
Accepted
10 April 2014

BACKGROUND AND PURPOSE

For decades, inhibitors of the cystic fibrosis transmembrane conductance regulator (CFTR) chloride channel have been used as tools to investigate the role and function of CFTR conductance in cystic fibrosis research. In the early 2000s, two new and potent inhibitors of CFTR, $CFTR_{inh}$-172 and GlyH-101, were described and are now widely used to inhibit specifically CFTR. However, despite some evidence, the effects of both drugs on other types of Cl^--conductance have been overlooked. In this context, we explore the specificity and the cellular toxicity of both inhibitors in CFTR-expressing and non–CFTR-expressing cells.

EXPERIMENTAL APPROACH

Using patch-clamp technique, we tested the effects of $CFTR_{inh}$-172 and GlyH-101 inhibitors on three distinct types of Cl^- currents: the CFTR-like conductance, the volume-sensitive outwardly rectifying Cl^- conductance (VSORC) and finally the Ca^{2+}-dependent Cl^- conductance (CaCC). We also explored the effect of both inhibitors on cell viability using live/dead and cell proliferation assays in two different cell lines.

KEY RESULTS

We confirmed that these two compounds were potent inhibitors of the CFTR-mediated Cl^- conductance. However,GlyH-101 also inhibited the VSORC conductance and the CaCC at concentrations used to inhibit CFTR. The $CFTR_{inh}$-172 did not affect the CaCC but did inhibit the VSORC, at concentrations higher than 5 μM. Neither inhibitor (20 μM; 24 h exposure) affected cell viability, but both were cytotoxic at higher concentrations.

CONCLUSIONS AND IMPLICATIONS

Both inhibitors affected Cl^- conductances apart from CFTR. Our results provided insights into their use in mouse models.

Abbreviations

CaCC, calcium-activated Cl^- conductance; CFTR, cystic fibrosis transmembrane conductance regulator; DCT, distal convoluted tubules; NPPB, 5-nitro-2-(3-phenylpropylamino)-benzoic acid; PCT, proximal convoluted tubules; VSORC, volume-sensitive outwardly rectifying Cl^- conductance

Introduction

The cystic fibrosis transmembrane conductance regulator (CFTR) is a glycoprotein expressed at the apical membrane of airway, gastrointestinal, renal and other epithelial cells, mutations of which cause the genetic disease cystic fibrosis. The CFTR is a cAMP-dependent Cl^- channel, but it also modulates other ion channels and transporters (Julien *et al.*, 1999;

Barriere *et al.*, 2003; L'Hoste *et al.*, 2009; Billet and Hanrahan, 2013; channel nomenclature follows Alexander *et al.*, 2013). CFTR dysfunction alters ion and fluid secretions in several organs and produces cystic fibrosis with lung disease, intestinal obstruction, pancreatic insufficiency and male infertility.

In the late 1980s, several patch-clamp studies described a Cl^- channel exhibiting low conductance (<10 pS) and activated by increased intracellular cAMP level (Gray *et al.*, 1988; Champigny *et al.*, 1990; Tabcharani *et al.*, 1990). Soon after, studies using the patch-clamp technique confirmed the ability of the protein CFTR to transport, selectively, Cl^- ions (Drumm *et al.*, 1990; Rich *et al.*, 1990). Since this important discovery, investigations of the role, function and structure/activity relationship of the CFTR Cl^- channel have concentrated on the discovery of selective inhibitors. After a screening of 200 compounds, Greger and colleagues identified two very potent inhibitors of CFTR-like Cl^- permeable conductances in kidney cells: diphenylamine-2-carboxylate (DPC; Di Stefano *et al.*, 1985) and 5-nitro-2-(3-phenylpropylamino)-benzoic acid (NPPB; Wangemann *et al.*, 1986). However, the specificity and efficacy of these inhibitors were highly dependent on the concentrations used and inhibited not only the CFTR conductance, but also other types of Cl^- conductances such as the volume-sensitive outwardly rectifying Cl^- conductance (VSORC), the calcium-activated Cl^- conductance (CaCC) or even members of the ClC family, such as ClC-2 (Furukawa *et al.*, 1998) and CLC-3 (Wang *et al.*, 2012). For more than a decade, these two inhibitors and other compounds such as glibenclamide, were routinely used to study the Cl^- selective CFTR channel (see Hwang and Sheppard, 1999).

In 2002, Verkman and colleagues identified the thiazolidinones as a new family of compounds that were able to inhibit more specifically CFTR in the micromolar range (Ma *et al.*, 2002). Among these, $CFTR_{inh}$-172 (3-[(3-trifluoromethyl)phenyl]-5-[(4-carboxyphenyl)methylene]-2-thioxo-4-thiazolidinone) was identified as the most potent and most specific reversible inhibitor for three CFTR-related functions: the epithelial iodide transport; the cellular Cl^- current; and the secretion of intestinal fluid. $CFTR_{inh}$-172 acts as an allosteric inhibitor, targeting the cytoplasmic face of the CFTR protein at its nucleotide-binding domain 1 and maintaining a closed state (Caci *et al.*, 2008) of the related Cl^- conductance. This inhibitor exhibited an IC_{50} around 300 nM that could rise to μM levels, in epithelial cells (Taddei *et al.*, 2004).

The same group identified glycine hydrazides as another class of CFTR inhibitors (Muanprasat *et al.*, 2004). N-(2-naphthalenyl)-((3,5-dibromo-2,4-dihydroxyphenyl) methylene)glycine hydrazide (GlyH-101), the most potent compound of this class, occludes the channel pore from the extracellular side, causes a voltage-dependent inhibition of CFTR current and transforms the CFTR-related linear current–voltage relationship in an inwardly rectifying curve when applied at 10 μM, with K_i values from 1.4 μM at +60 mV to 5.6 μM at −60 mV (Muanprasat *et al.*, 2004). This inhibitor was defined as an open-channel blocker of CFTR and was more water-soluble than $CFTR_{inh}$-172 (~1 mM for GlyH-101 and only 20–50 μM for $CFTR_{inh}$-172) making it a better tool for further pharmacological investigations of the CFTR (Barman *et al.*, 2011; Stahl *et al.*, 2012; Fisher *et al.*, 2013; Rubera *et al.*, 2013).

The effectiveness, *in vivo*, of both $CFTR_{inh}$-172 and a derivative of GlyH-101 was established through their inhibition of cholera toxin-induced intestinal fluid secretion (Thiagarajah *et al.*, 2004) and of CFTR-dependent cyst growth in a mouse model of autosomal dominant polycystic kidney disease (Yang *et al.*, 2008). They are now widely used in cystic fibrosis research to investigate in detail the role of CFTR in various cell types and/or organs (Sondo *et al.*, 2011; Lu and Ding, 2012).

However, the wide range of concentrations used, varying from 20 μM (Bijvelds *et al.*, 2009) up to 100 μM (Baniak *et al.*, 2012) for $CFTR_{inh}$-172 and from 20 μM (Illek *et al.*, 2008) up to 50 μM (Zhang *et al.*, 2010; Muanprasat *et al.*, 2013) for GlyH-101, give rise to many concerns about specificity and the 'appropriate concentrations to use' for these compounds. Therefore, we conducted a study to test the efficacy (concentration-dependency) and specificity of these widely used CFTR inhibitors on various types of Cl^- currents already identified and described in different cell lines (Barriere *et al.*, 2003; l'Hoste *et al.*, 2010). Briefly, the putative inhibitory effect of both inhibitors on the ubiquitous VSORC conductance was tested in CFTR-expressing cells (kidney cell line), as well as in non–CFTR-expressing cells (PS120 cell line). We also explored the effect of $CFTR_{inh}$-172 and GlyH-101 on the CaCC conductance in the kidney cell model.

Using the patch-clamp technique, we first confirmed that these two compounds are potent inhibitors of the CFTR-mediated Cl^- conductance. However, we also found that GlyH-101 inhibited two other Cl^--conductance types (VSORC and CaCC) at almost the same concentration as that used to inhibit CFTR, raising concerns about its ability to selectively inhibit the CFTR-mediated conductance in a multicomponent Cl^- channel biological system. $CFTR_{inh}$-172 was similarly lacking in specificity, as we observed inhibition of VSORC-mediated conductance with this compound when used in concentrations greater than 5 μM. We finally tested the cellular toxicity of these inhibitors. We discuss the implication of these finding for studies of the pathophysiology of CFTR channels.

Methods

Culture of kidney cells

For the CFTR-expressing cell model, we used immortalized cell lines of murine renal distal convoluted tubules (DCT) or proximal convoluted tubules (PCT) (Barriere *et al.*, 2003; Milosavljevic *et al.*, 2010; Peyronnet *et al.*, 2012). For the non–CFTR-expressing cells, we used PS120 cell line (a cell line derived from hamster CCL39 fibroblasts) lacking the *cftr* gene (Barriere *et al.*, 2001; Milosavljevic *et al.*, 2010). Cultures were maintained in a water-saturated atmosphere of 5% CO_2/95% air at 37°C.

Electrophysiological studies

The ruptured whole-cell configuration of the patch-clamp technique was used to assess the functional expression of CFTR and to measure other Cl^- conductances. Cell currents

and cell capacitances were recorded using an EPC 10 amplifier [HEKA Elektronik, Lambrecht (Pfalz), Germany]. Cells were held at –40 mV, and 400 ms pulses from –100 to +100, +120 or +140 mV were applied in 20 mV increments. I/V relationships were expressed as mean current amplitudes measured at all potentials at 50 or 350 ms after the pulse onset. The offset potentials between both electrodes were zeroed before sealing and corrected for liquid junction potentials as previously described (Duranton *et al.*, 2002).

The pipette solution contained (in mM): 140 NMDGCl, 10 HEPES (pH 7.4, HCl), 5 EGTA and 5 MgATP (290 mOsm kg^{-1} H_2O). The normal NMDGCl bath solution contained (in mM): 140 NMDGCl, 10 HEPES (pH 7.4, HCl), 1 $CaCl_2$, 1 $MgCl_2$, 30–40 mannitol (320–330 mOsm kg^{-1} H_2O). This solution was designed to avoid spontaneous activation of VSORC currents. Hypoosmotic NMDGCl solution (285–290 mOsm kg^{-1} H_2O) was obtained by removing the mannitol from the normal NMDGCl bath solution.

Cell viability/cytotoxicity assay kit

The LIVE/DEAD® Cell Viability/Cytotoxicity Assay Kit (Invitrogen, Saint-Aubin, France) was used on cells after 24 h of incubation with CFTR inhibitors, cultured with 1% serum. Using this kit, living cells showed green fluorescence (detecting calcein-acetoxymethyl ester) and dead cells showed red fluorescence (detecting homodimeric ethidium bromide). Cells were visualized with a Carl Zeiss Axiovert D1 inverted microscope using a 40× LD Plan-Neofluar objective (Carl Zeiss SAS, LE Peck, France). Images were recorded using an Axiocam MRm (Carl Zeiss SAS), and quantification of green and red fluorescence was performed using individual pixel quantification with ImageJ software (NIH, Bethesda, MD, USA) on three independent micrographs per well.

MTT assays

The MTT assay is based on the transformation of 3-(4,5-dimethylthiazol-2-yl)-2,5-diphenyltetrazolium bromide in formazan by mitochondrial dehydrogenase allowing estimation of cell viability. Cells cultured in a 48-well plate (1% serum) and exposed for 24 h to CFTR inhibitors, were rinsed once with PBS and incubated for 1 h (37°C, 5% CO_2) into a DMEM:F12 culture medium without phenol red, supplemented with 5% serum and 0.5 mg mL^{-1} of MTT. Cells were then lysed (SDS 10%, HCl 0.01N) and maintained overnight in the same condition. Optical density measurements were performed at 562 nm, using a Biotek microplate reader. Lysates of eight independent conditions were prepared and two MTT assays were performed for each condition.

Data analysis

Statistical analysis was performed using R software (R Development Core Team (2011). R: A language and environment for statistical computing. R Foundation for Statistical Computing, Vienna, Austria. ISBN 3-900051-07-0, URL http://www.R-project.org/). Dose–response relationships for each experimental condition were fitted with the Hill equation using SigmaPlot software (Systat Software, San Jose, CA, USA) to calculate IC_{50} values. $P < 0.05$ was accepted to show significant differences between means.

Materials

All chemical compounds were provided by Sigma Aldrich except for GlyH-101 compound (Merck Millipore Darmstadt, Germany).

Results

To study the effects of $CFTR_{inh}$-172 and GlyH-101 on cell viability and the putative inhibitory effect of both substances on three different chloride channel types, we used CFTR-expressing cells (epithelial kidney cells originating from proximal or distal convoluted segments, PCT or DCT) and non–CFTR-expressing cells (PS120 cells). In these kidney cell models, a CFTR-mediated conductance, a VSORC and a CaCC have been described in detail, previously (Barriere *et al.*, 2003; L'Hoste *et al.*, 2009).

Cellular toxicity of the $CFTR_{inh}$-172 and GlyH-101 inhibitors on CFTR-expressing and non–CFTR-expressing cells

We first evaluated the cytotoxicity of $CFTR_{inh}$-172 and GlyH-101 in kidney cells. Confluent cell cultures were exposed to increasing concentrations of GlyH-101 and $CFTR_{inh}$-172 (1–50 μM), and the fluorescent dye assay used to determine cytotoxicity (live/dead labelling) after incubation for 24 h. Figure 1A illustrates confluent cell monolayers in the absence and presence of $CFTR_{inh}$-172 (upper part) or GlyH-101 (lower part). From 1 to 20 μM, $CFTR_{inh}$-172 and GlyH-101 had no significant effect on cell viability as indicated by a homogeneous green labeling of the monolayers (Figure 1A and B). However at a higher concentration (50 μM), both substances induced cell death as revealed by the decrease of green-labelled areas and a simultaneous increase in red positive cells (dead cells). To confirm the toxicity of both substances, we performed MTT assays on confluent CFTR-expressing cells monolayers. These experiments confirmed for both substances a dramatic decrease of the cell viability at 50 μM but revealed also a marked effect for lower concentrations (20 μM and even 10 μM, Figure 1C). MTT assays were also performed on non–CFTR-expressing PS120 cells. GlyH-101 also decreased cell viability (Figure 1D) at concentrations higher than 5 μM. Interestingly, CFTRinh-172 was more cytotoxic than GlyH-101 and exhibited a significant effect at 5 μM.

Specificity and efficacy of $CFTR_{inh}$-172 and GlyH-101 inhibitors on CFTR-like conductances

To record only the CFTR-like Cl^- conductance in the CFTR-expressing cell model, the endogenous CaCC-mediated current was impaired by the use of a high concentration of EGTA in the pipette solution and the extracellular bath solution was adjusted to 320 mosmol kg^{-1} H_2O (addition of mannitol) to avoid activation of the VSORC conductance (Barriere *et al.*, 2003). Under these experimental conditions, perfusion of forskolin (1–10 μM) rapidly induced (<4 min) the activation of a Cl^- current exhibiting a linear current/voltage relationship (Figure 2A–C). Once the forskolin-activated current had reached a maximum, $CFTR_{inh}$-172 or GlyH-101 were per-

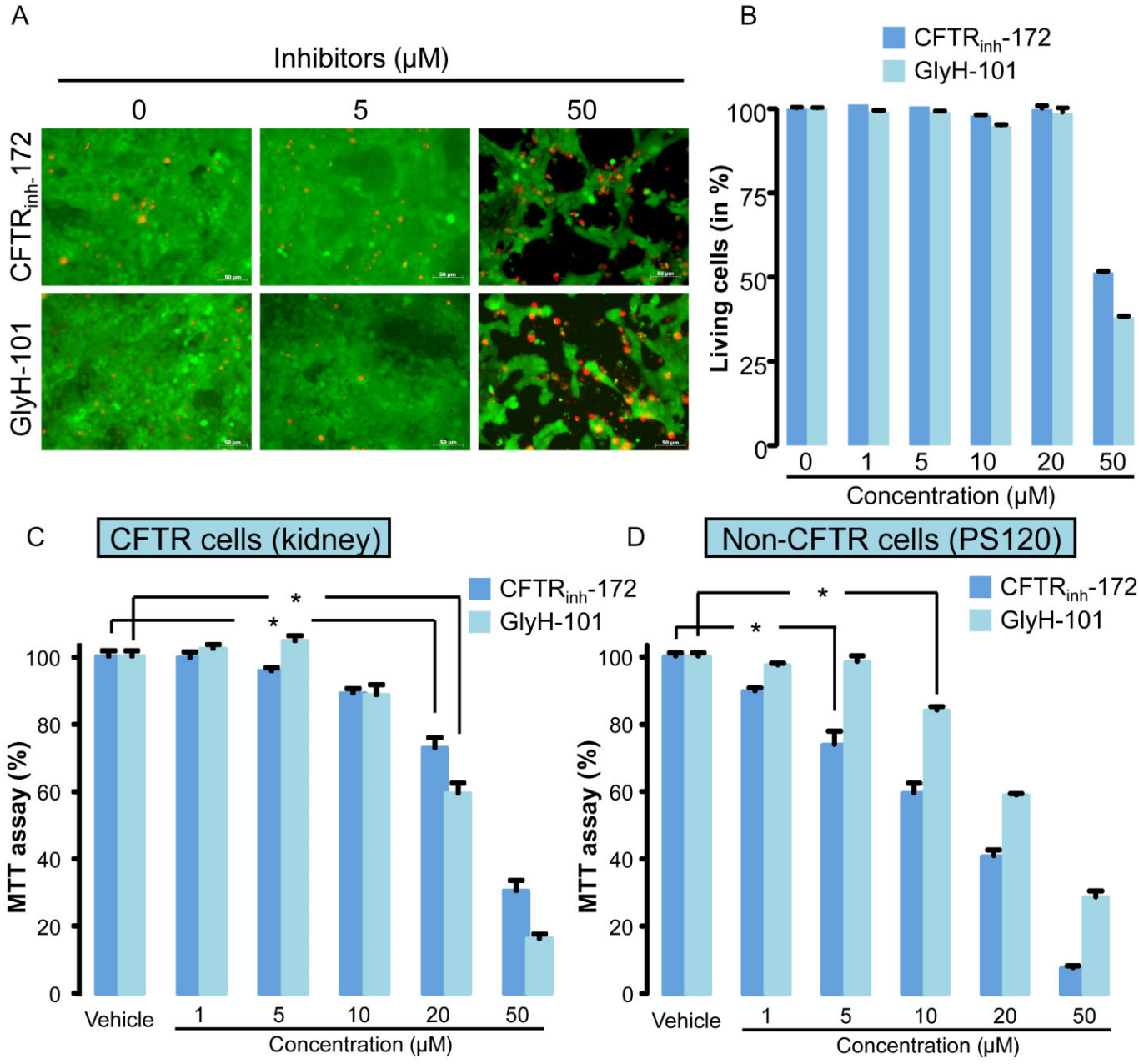

Figure 1

Effect of CFTR$_{inh}$-172 and GlyH-101 inhibitors on cellular toxicity. (A and B). Representative fluorescent dye staining (A) and related quantification of cell death (B) in CFTR-expressing cells (confluent kidney PCT cell monolayers) exposed for 24 h to increasing concentrations of CFTR$_{inh}$-172 or GlyH-101 (concentrations ranging from 0.5 to 50 μM). Live cells labelled with calcein-AM appeared green while dead cells labelled with homodimeric propidium iodide appeared red. Scale bars represents 80 μm. Values were normalized to the 100% of live cells in control experiments and were means (±SEM) of three to six individual experiments. (C) MTT assay performed on CFTR-expressing cells (kidney PCT cells) exposed as in (A) to increasing concentrations of both CFTR inhibitors. Values were normalized to control experiments and represent means (±SEM) of eight individual experiments. (D) MTT assay performed on non–CFTR-expressing cells (PS120) exposed to increasing concentrations of both inhibitors. Values were normalized to vehicle experiments and represent means (SEM) of eight individual experiments. *$P < 0.05$, Tukey's HSD test.

fused at increasing concentrations (0.5, 1, 5, 10 μM, Figure 2A and B). CFTR$_{inh}$-172 induced a reversible concentration-dependent inhibition of the CFTR-like current that was maximal at 5 μM (Figure 2A and D). Similarly, GlyH-101 induced a concentration-dependent inhibition of the CFTR-like current (Figure 2B and E). This inhibition was partly reversible on washing the cells (70% of recovery within 4 min) and showed a significant potential dependency (at

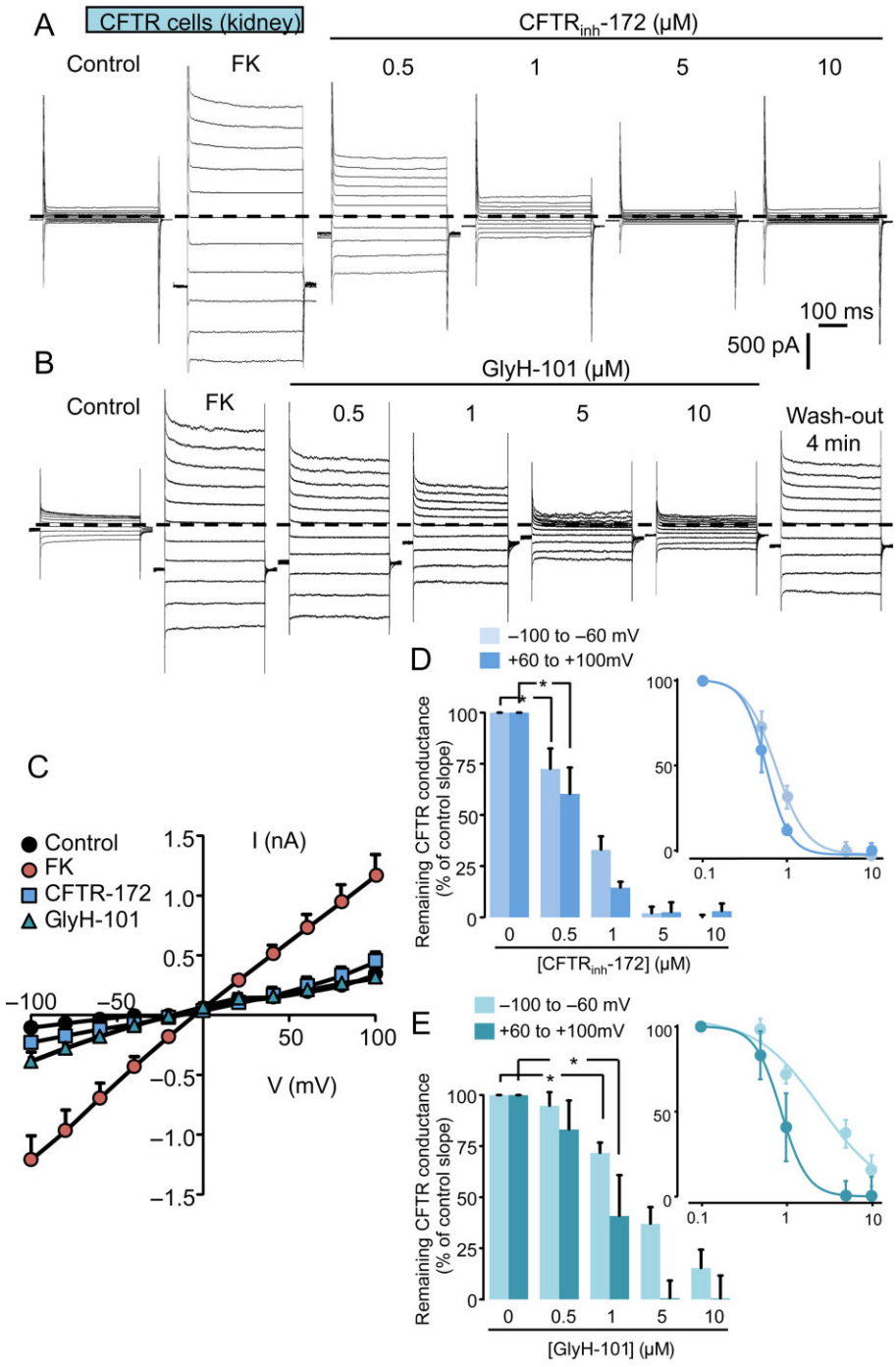

Figure 2

Inhibition of forskolin-activated CFTR-like conductance by CFTR$_{inh}$-172 and GlyH-101 inhibitors in CFTR-expressing cells. (A and B) Whole-cell current traces recorded in CFTR-expressing cells (kidney, DCT cells) under control condition and after forskolin exposure (FK, 1–10 μM). Once the Cl^- conductance is fully developed (3–4 min), CFTR$_{inh}$-172 or GlyH-101 were perfused at increasing concentrations (0.5, 1, 5, 10 μM). The membrane potential was held at –40 mV and currents were elicited by a train of 11 voltage steps (400 ms duration) between –100 and +100 mV in +20 mV increment. The zero current level is indicated by a dashed line. (C) Mean current/voltage relationships measured at 350 ms after the onset pulse corresponding to experiments performed (A and B) under control condition, after FK exposure and finally in the presence of CFTR$_{inh}$-172 (10 μM) or GlyH-101 (10 μM). Values are means (±SEM) of six to eight individual cells. (D and E) Histograms illustrating the concentration-dependent inhibition of the CFTR conductance obtained with increasing concentrations of CFTR$_{inh}$-172 (D) or GlyH-101 (E). Concentrations of both inhibitors vary from 0.5 up to 10 μM as indicated. Values were individually normalized for each concentration of inhibitors to the maximal current slope (recorded after FK stimulation) calculated between –100 and –60 mV and between +60 and +100 mV. Values are means (±SEM) of five to eight individual cells. *$P < 0.05$, Tukey's HSD test. The insets show the logarithmic dose–response curves corresponding to each inhibitor.

10 μM, the inhibition was more pronounced at positive potentials than at negative potentials, Figure 2B, C and E). Figure 2D and E summarises the inhibition for each concentration of the inhibitors. Values are expressed as a function of CFTR-maximal current slope (current slopes were calculated between −100 and −60 mV and between +60 and +100 mV). The concentration–response curve revealed an IC_{50} value below 1μM for $CFTR_{inh}$-172 (0.74 and 0.56 μM for negative and positive potentials respectively) and varying between 3 μM at negative potentials and 0.87 μM at positive potentials for GlyH101. These results confirmed the ability of both drugs to inhibit efficiently the CFTR-mediated Cl^- currents in mouse kidney cells.

Sensitivity of the VSORC to $CFTR_{inh}$-172 and GlyH-101 inhibitors

Next we looked for the effects of $CFTR_{inh}$-172 and GlyH-101 inhibitors on the VSORC in CFTR-expressing and non–CFTR-expressing cells. As expected, exposing both cell models to a hypo-osmotic shock (through a decrease of external osmotic pressure from 320–330 to 290 mosmol kg^{-1} H_2O) induced outwardly rectifying currents exhibiting a time-dependent inactivation at depolarizing potentials (Figure 3A and B). Once this activated conductance was stable, cells were exposed to increasing concentrations of $CFTR_{inh}$-172 (Figure 3A and B). In CFTR-expressing cells, $CFTR_{inh}$-172 did not affect this conductance up to 1 μM but, at 10 μM, partly and reversibly inhibited the VSORC (Figure 3A and C, ~50% of inhibition at negative and positive potentials). The non-specific inhibitor of Cl^- conductance NPPB (100 μM) completely inhibited the remaining fraction of the VSORC current. Similarly in non–CFTR-expressing cells, $CFTR_{inh}$-172 inhibited also the VSORC current in a concentration-dependent manner (Figure 3B and D). Figure 3E and F illustrates the percentage of inhibition of the VSORC conductance for increasing concentrations of $CFTR_{inh}$-172 measured at negative (from −100 to −60 mV, Figure 3E) and positive potentials (from +60 to +100 mV, Figure 3F), in CFTR-expressing and non–CFTR-expressing cells. In CFTR-expressing cells, $CFTR_{inh}$-172 exhibited an IC_{50} of 12 μM towards VSORC-mediated Cl^- currents either at negative or positive potentials. In non–CFTR-expressing cells, the calculated IC_{50} was 5.33 μM, independent of applied potential.

Similar experiments were performed on the VSORC conductance using the GlyH-101 inhibitor. As shown in Figure 4A and B, in CFTR-expressing cells, GlyH-101 was a very potent and reversible inhibitor of the VSORC conductance and exhibited a greater efficacy than $CFTR_{inh}$-172, with significant inhibition at 0.5 μM and almost total blockade at 10 μM (Figure 4A and B). The IC_{50} was calculated to be about 1 μM (0.87 and 1.07 μM for negative and positive potentials, respectively) and suggested an inhibitory effect independent of the membrane potential (Figure 4E and F). In non–CFTR-expressing cells, GlyH-101 also inhibited the VSORC current (Figure 4C and D) with an IC_{50} of 5.38 and 6.26 μM at negative and positive potentials respectively (Figure 4E and F). Altogether, the inhibition of VSORC conductance by CFTRinh-172 and GlyH-101 in both cell models suggested a direct action of both compounds on the channel pore.

Sensitivity of the CaCC to $CFTR_{inh}$-172 and GlyH-101 inhibitors

Next, we evaluated the inhibitory effects of $CFTR_{inh}$-172 and GlyH-101 on the CaCC in the two cell models. As already demonstrated in CFTR-expressing cells (Barriere *et al.*, 2003), ionomycin (2 μM) stimulated an outwardly rectifying Cl^- conductance exhibiting a time-dependent activation at depolarizing potentials (Figure 5A–C). Once the current had reached a maximum (3–6 min), cells were exposed to increasing concentrations of $CFTR_{inh}$-172 (Figure 5A) and GlyH-101 (Figure 5B). $CFTR_{inh}$-172 did not affect the CaCC up to 10 μM (Figure 5A, C and D). Interestingly, GlyH-101 was without effect at the lowest concentration (0.5 μM, not shown), but significantly reduced Ca^{2+}-activated Cl^- current at higher concentrations (Figure 5B, C and D). When applied at 10 μM, GlyH-101 blocked more than 70% (n = 5) of the CaCC conductance (slope current calculated between +60 and +100 mV, Figure 5D). The concentration–response curve revealed an IC_{50} of 3.38 μM for positive potentials.

Discussion and conclusion

In this study we have evaluated the putative inhibitory effects of two CFTR inhibitors ($CFTR_{inh}$-172 and GlyH-101) on three well-described Cl^--mediated conductances: CFTR, the volume-activated Cl^- conductance (VSORC) and the CaCC. As expected, both inhibitors totally inhibited the forskolin-activated CFTR Cl^- conductance with an IC_{50} in the micromolar range. GlyH-101 induced a specific profile of inhibition of the CFTR-mediated conductance with a more pronounced inhibition at positive potentials than at negative potentials. However, the inward rectification induced by 5 or 10 μM of GlyH-101 was much less pronounced than previously demonstrated (Muanprasat *et al.*, 2004). This minor difference might be partially explained by a difference in the sensitivity and biophysical properties between mouse CFTR and human CFTR (Muanprasat *et al.*, 2004).

Besides the inhibition of CFTR conductance, we also demonstrated that GlyH-101 inhibited two other types of Cl^- conductances (VSORC and CaCC) at concentrations close to those used to inhibit CFTR conductance. We also observed a significant inhibition of CaCC at low concentrations of GlyH-101 which was in agreement with an earlier report that GlyH-101 inhibited ionomycin-induced I^- fluxes driven by TMEM16A protein [the main constituent of the CaCC (Caputo *et al.*, 2008)]. This inhibition reached more than 60% with 20 μM of GlyH-101. This sensitivity of the CaCC to GlyH-101 was also reported at a higher concentration (50 μM) in cells expressing human CFTR (Muanprasat *et al.*, 2004). The other non-CFTR conductance examined, VSORC-was also inhibited (Figure 4) at low concentrations of GlyH-101 with an almost complete inhibition of the current at 10 μM. The use of non–CFTR-expressing cells demonstrated the direct action of GlyH-101 on the VSORC. This is an important finding as a link between CFTR expression and VSORC activity in several cell lines has already been demonstrated (Vennekens *et al.*, 1999; Ando-Akatsuka *et al.*, 2002). Taken together, the demonstration that GlyH-101 inhibits VSORC and CaCC at almost the same concentrations

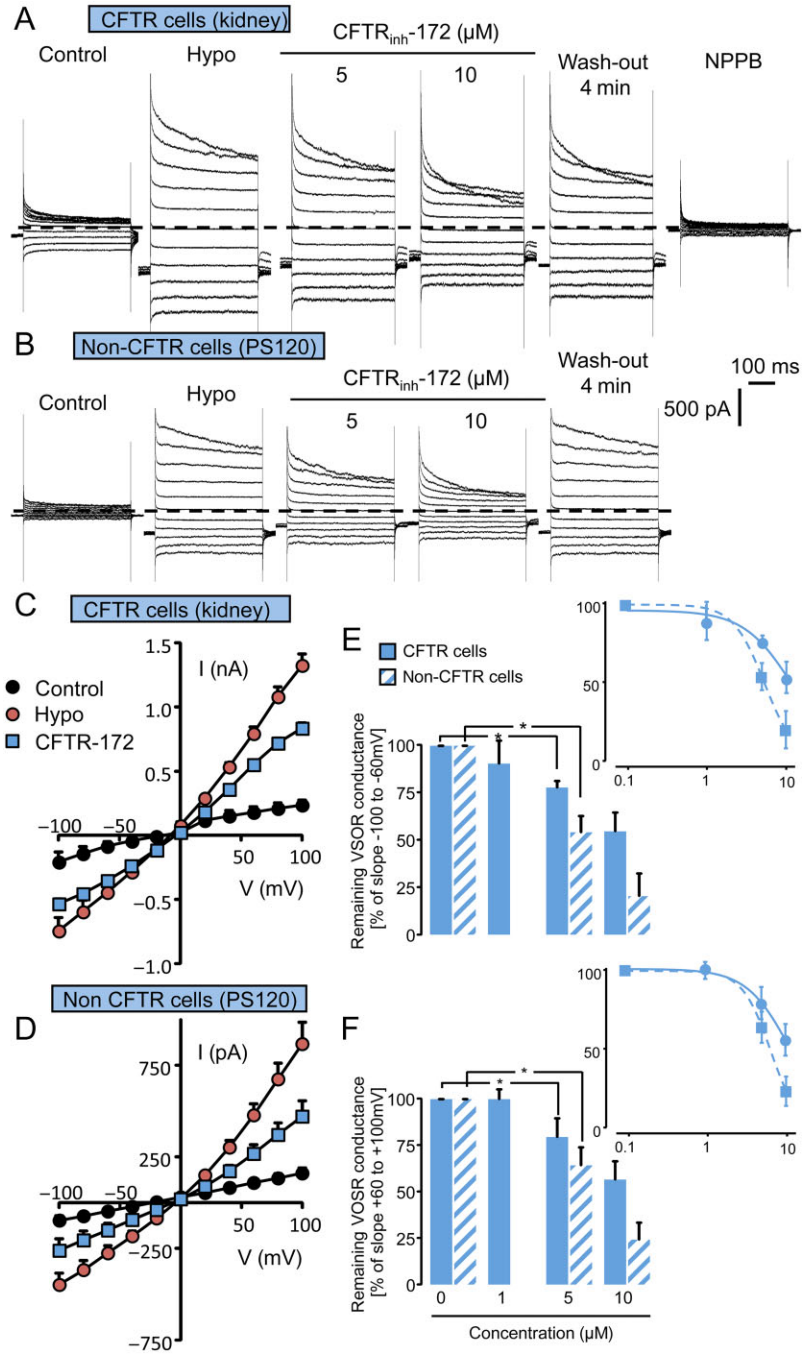

Figure 3

Effects of CFTR$_{inh}$-172 on the VSORC measured in CFTR-expressing cells (kidney) and in non–CFTR-expressing cells (PS120). (A and B) Whole-cell currents recorded in CFTR-expressing cells (A) and in non–CFTR-expressing cells (B). Cl^- currents were recorded in control conditions and after replacing the hypertonic bath by a hypotonic solution (hypo). Once the Cl^- conductance is fully developed (3–4 min), CFTR$_{inh}$-172 was perfused (5, 10 μM as indicated). Normal bath solution was made hypertonic (340 mOsmol including 30–40 mOsm of Mannitol), and the hypotonic one was adjusted by removing mannitol from the normal bath solution (290 mOsm). NPPB (100 μM) completely inhibited swelling-activated Cl^- current. The membrane potential was held at –40 mV and currents were elicited by a train of 11 voltage steps (400 ms duration) between –100 and +100 mV in +20 mV increment. (C and D) Mean current/voltage relationships measured in CFTR-expressing cells (C) and in non–CFTR-expressing cells (D) recorded in control condition, after the stabilization of the VSORC Cl^- current (hypo) and in the presence of CFTR$_{inh}$-172 (10 μM). Current values were measured 5 ms after the onset pulse. Values are means (±SEM) of five to six individual cells. (E and F) Histogram illustrating the remaining fraction of the VSORC conductance for increasing concentrations of CFTR$_{inh}$-172 (1, 5, 10 μM) measured in CFTR-expressing cells and in non–CFTR-expressing cells. Values were individually normalized for each concentration of CFTR$_{inh}$-172 to the maximal current slope (recorded after hypotonic solution exposure) calculated between –100 and –60 mV (E) and between +60 and +100 mV (F). Values are means (±SEM) of five to six individual cells. *P < 0.05, Tukey's honestly significant difference test. The insets show the logarithmic dose–response curves calculated between –100 and –60 mV (E) and between +60 and +100 mV (F).

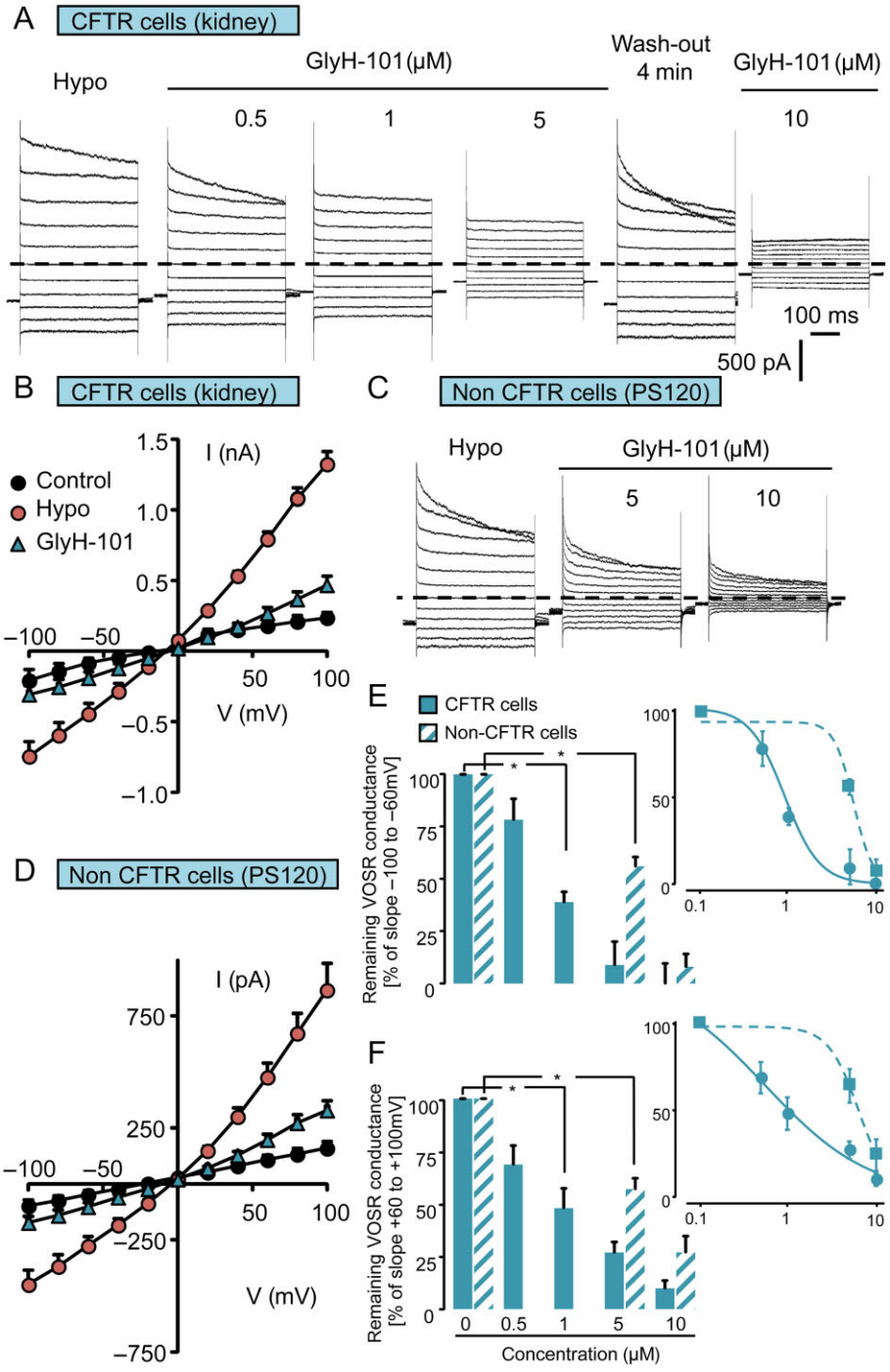

Figure 4

Effects of GlyH-101 on VSORC conductance measured in CFTR-expressing cells (kidney) and in non–CFTR-expressing cells (PS120). (A and C) Whole-cell current traces recorded in CFTR-expressing cells (A) and in non–CFTR-expressing cells (C) in control condition and after replacing the hypertonic bath by a hypotonic solution (hypo). Once the Cl^- conductance is fully developed, GlyH-101 was perfused at increasing concentrations (0.5, 1, 5, 10 μM) as indicated. The membrane potential was held at –40 mV and currents were elicited by a train of 11 voltage steps (400 ms duration) between –100 and +100 mV in +20 mV increments. (B and D) Means current/voltage relationships measured in CFTR-expressing cells (B) and in non–CFTR-expressing cells (D) recorded in control conditions, after the stabilization of the VSORC Cl^- current (hypo) and in the presence of GlyH-101 (10 μM). Currents values were measured 5 ms after the onset pulse. Values are means (±SEM) of five to six individual cells. (E and F) Histogram illustrating the remaining fraction of the VSORC conductance for increasing concentrations of GlyH-101 (0.5, 1, 5, 10 μM) measured in CFTR-expressing cells and in non–CFTR-expressing cells. Values were individually normalized for each concentration of GlyH-101 to the maximal current slope (recorded after hypotonic solution exposure) calculated between –100 and –60 mV (E) and between +60 and +100 mV (F). Values are means (±SEM) of five to six individual cells. *$P < 0.05$, Tukey's HSD test. The insets show the logarithmic dose–response curves calculated between –100 and –60 mV (E) and between +60 and +100 mV (F).

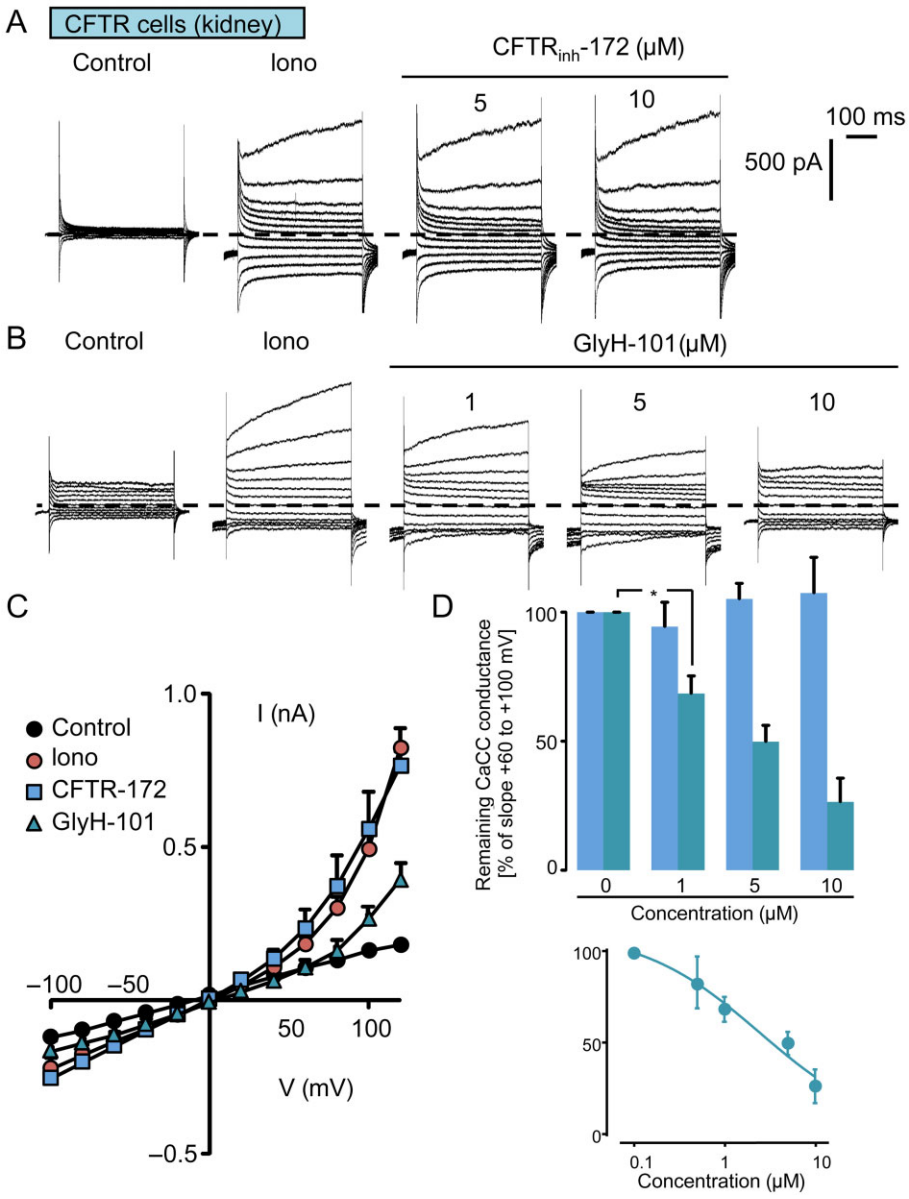

Figure 5

Effects of CFTR$_{inh}$-172 and GlyH-101 inhibitors on the CaCC. (A and B) Whole-cell current traces recorded in CFTR-expressing cells (kidney) in control conditions and after ionomycin treatment (iono, 2 μM). Once the CaCC is fully developed (<5 min), CFTR$_{inh}$-172 (A) or GlyH-101 (B) were perfused at increasing concentrations (1, 5, 10 μM). The membrane potential was held at –40 mV and currents were elicited by a train of 12 voltage steps (400-ms duration) between –100 and +120 mV in +20 mV increments. (C) Mean current/voltage relationships measured at 350 ms after the onset pulse corresponding to experiments performed as in (A) and (B) under control conditions, after ionomycin exposure and finally in the presence of GlyH-101 (10 μM) or CFTR$_{inh}$-172 (10 μM). Values are means (±SEM) of five to six individual cells. (D) Histogram illustrating the remaining fraction of the CaCC conductance as a function of GlyH-101 or CFTR$_{inh}$-172 concentrations (1, 5, 10 μM). Values measured for each concentration were individually normalized to the maximal current slope measured between +60 and +120 mV in the absence of any inhibitor. Values are means (±SEM) of five to six individual cells. *P < 0.05, Tukey's HSD test. The insets show the logarithmic dose–response curve for GlyH-101 and calculated between –100 and –60 mV (E) and between +60 and +120 mV (F).

(5–10 μM) as used to fully inhibit CFTR, raises serious questions about its specificity and excludes this compound from future investigations as a means of clearly distinguishing CFTR-mediated conductance in a multicomponent Cl^- channel conductance analysis.

Concerning CFTR$_{inh}$-172, we noted that a concentration of 5 μM induced a full inhibition of the CFTR conductance along with no noticeable inhibition of the CaCC [as previously observed (Caputo *et al.*, 2008)] but a noticeable, but moderate, inhibition (from ~15 to 50% depending on the cell

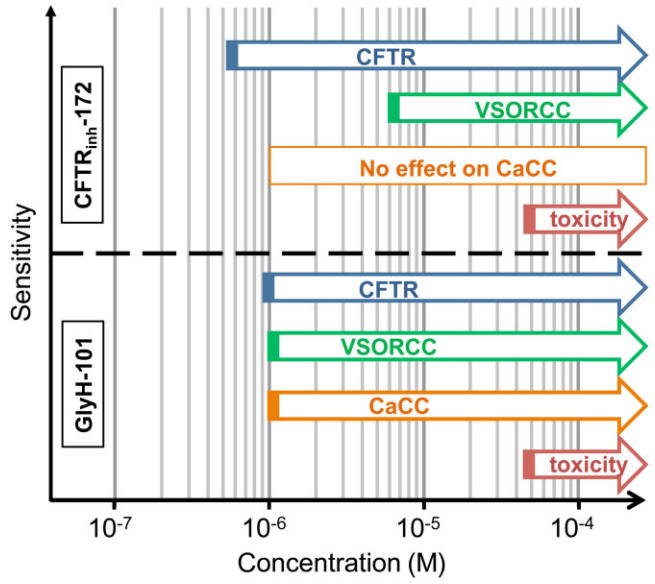

Figure 6

Schematic representation of the specificity of CFTR$_{inh}$-172 and GlyH-101 towards Cl^- conductances, depending on the concentration used.

type) of the VSORC. We conclude that, low concentrations of CFTR$_{inh}$-172 (<10 μM) might represent the best experimental condition to provide fully inhibition of the CFTR conductance, with minimum effects on other Cl^- conductances. Figure 6 summarises the concentration ranges of CFTR$_{inh}$-172 and GlyH-101 used by us and their corresponding effects on CFTR, VSORC and CaCC conductances, expressed in mouse kidney epithelial cells.

Our data obtained on the efficacy of CFTR$_{inh}$-172 and GlyH-101 apply only to mouse models, as a recent study (Stahl *et al.*, 2012) using different CFTR orthologs, originating from human, killifish, pig and shark, disclosed a marked species-related difference in sensitivity to CFTR$_{inh}$-172. For example, in the oocyte expression system, the shark 'CFTR-like' protein was almost insensitive to CFTR$_{inh}$-172 (10% of inhibition at 25 μM) while the human CFTR was only inhibited by ~50% at 20 μM. Therefore, we could surmise the inhibitory effects of CFTR$_{inh}$-172 and GlyH-101 would also be different between the different orthologues of the proteins supporting the CaCC (mainly members of the TMEM16 family) and the VSORC conductances.

Besides the effects of both inhibitors on CFTR and non-CFTR Cl^- conductances, CFTR$_{inh}$-172 and GlyH-101 also impaired mitochondrial function in cell lines, devoid of CFTR (Kelly *et al.*, 2010). These authors demonstrated that CFTR$_{inh}$-172 and GlyH-101 induced, within 30 min, a significant increase in the production of reactive oxygen species, starting at a low concentration, 0.2 μM, for both inhibitors and correlated with a fall in the mitochondrial membrane potential. However, in spite of this evidence for impaired mitochondrial function, this effect does not seem to be related to short term toxicity, as both compounds were cytotoxic only at high concentration (~50 μM, Figure 1). Nevertheless, this non-specific effect raises important concerns for the potential therapeutic applications of these compounds.

Finally, for CFTR$_{inh}$-172, a concentration of 5 μM is probably the best to fully and selectively inhibit CFTR conductance, without affecting other type of Cl^- conductances (i.e. VSORC and the CaCC) or cell viability. In conclusion, investigators should be wary of the non-selectivity of GlyH-101 (and to a lesser extent, of CFTRinh-172) in order not to falsely attribute effects only to inhibition of CFTR.

Acknowledgements

We thank Professor Counillon L. (University of Nice-Sophia Antipolis, LP2M CNRS-UMR7370) for providing PS120 cell line. This study was supported by the French Association AFM (S Bendahhou).

Author contributions

N Mélis, M Tauc, M Cougnon, S Bendahhou, S Giuliano, I Rubera, C Duranton performed cellular experiments. M Tauc, S Bendahhou, C Duranton performed patch-clamp experiments. N Mélis, M Tauc, I Rubera, C Duranton wrote the paper with input and discussion from all of the co-authors.

Conflict of interest

The authors declare that they have no conflicts of interest to disclose.

References

Alexander SPH, Benson HE, Faccenda E, Pawson AJ, Sharman JL, Catterall WA *et al.* (2013). The Concise Guide to PHARMACOLOGY 2013/14: Ion Channels. Br J Pharmacol 170: 1607–1651.

Ando-Akatsuka Y, Abdullaev IF, Lee EL, Okada Y, Sabirov RZ (2002). Down-regulation of volume-sensitive Cl^- channels by CFTR is mediated by the second nucleotide-binding domain. Pflugers Arch 445: 177–186.

Baniak N, Luan X, Grunow A, Machen TE, Ianowski JP (2012). The cytokines interleukin-1beta and tumor necrosis factor-alpha stimulate CFTR-mediated fluid secretion by swine airway submucosal glands. Am J Physiol Lung Cell Mol Physiol 303: L327–L333.

Barman PP, Choisy SC, Gadeberg HC, Hancox JC, James AF (2011). Cardiac ion channel current modulation by the CFTR inhibitor GlyH-101. Biochem Biophys Res Commun 408: 12–17.

Barriere H, Poujeol C, Tauc M, Blasi JM, Counillon L, Poujeol P (2001). CFTR modulates programmed cell death by decreasing intracellular pH in Chinese hamster lung fibroblasts. Am J Physiol Cell Physiol 281: C810–C824.

Barriere H, Belfodil R, Rubera I, Tauc M, Poujeol C, Bidet M *et al.* (2003). CFTR null mutation altered cAMP-sensitive and

swelling-activated Cl^- currents in primary cultures of mouse nephron. Am J Physiol Renal Physiol 284: F796–F811.

Bijvelds MJ, Bot AG, Escher JC, De Jonge HR (2009). Activation of intestinal Cl^- secretion by lubiprostone requires the cystic fibrosis transmembrane conductance regulator. Gastroenterology 137: 976–985.

Billet A, Hanrahan JW (2013). The secret life of CFTR as a calcium-activated chloride channel. J Physiol 591 (Pt 21): 5273–5278.

Caci E, Caputo A, Hinzpeter A, Arous N, Fanen P, Sonawane N *et al.* (2008). Evidence for direct CFTR inhibition by CFTR(inh)-172 based on Arg347 mutagenesis. Biochem J 413: 135–142.

Caputo A, Caci E, Ferrera L, Pedemonte N, Barsanti C, Sondo E *et al.* (2008). TMEM16A, a membrane protein associated with calcium-dependent chloride channel activity. Science 322: 590–594.

Champigny G, Verrier B, Gerard C, Mauchamp J, Lazdunski M (1990). Small conductance chloride channels in the apical membrane of thyroid cells. FEBS Lett 259: 263–268.

Di Stefano A, Wittner M, Schlatter E, Lang HJ, Englert H, Greger R (1985). Diphenylamine-2-carboxylate, a blocker of the Cl(–)-conductive pathway in Cl(–)-transporting epithelia. Pflugers Arch 405 (Suppl. 1): S95–S100.

Drumm ML, Pope HA, Cliff WH, Rommens JM, Marvin SA, Tsui LC *et al.* (1990). Correction of the cystic fibrosis defect *in vitro* by retrovirus-mediated gene transfer. Cell 62: 1227–1233.

Duranton C, Huber SM, Lang F (2002). Oxidation induces a Cl(–)-dependent cation conductance in human red blood cells. J Physiol 539 (Pt 3): 847–855.

Fisher JT, Tyler SR, Zhang Y, Lee BJ, Liu X, Sun X *et al.* (2013). Bioelectric characterization of epithelia from neonatal CFTR knockout ferrets. Am J Respir Cell Mol Biol 49: 837–844.

Furukawa T, Ogura T, Katayama Y, Hiraoka M (1998). Characteristics of rabbit ClC-2 current expressed in Xenopus oocytes and its contribution to volume regulation. Am J Physiol 274 (2 Pt 1): C500–C512.

Gray MA, Greenwell JR, Argent BE (1988). Secretin-regulated chloride channel on the apical plasma membrane of pancreatic duct cells. J Membr Biol 105: 131–142.

Hwang TC, Sheppard DN (1999). Molecular pharmacology of the CFTR Cl^- channel. Trends Pharmacol Sci 20: 448–453.

Illek B, Fu Z, Schwarzer C, Banzon T, Jalickee S, Miller SS *et al.* (2008). Flagellin-stimulated Cl^- secretion and innate immune responses in airway epithelia: role for p38. Am J Physiol Lung Cell Mol Physiol 295: L531–L542.

Julien M, Verrier B, Cerutti M, Chappe V, Gola M, Devauchelle G *et al.* (1999). Cystic fibrosis transmembrane conductance regulator (CFTR) confers glibenclamide sensitivity to outwardly rectifying chloride channel (ORCC) in Hi-5 insect cells. J Membr Biol 168: 229–239.

Kelly M, Trudel S, Brouillard F, Bouillaud F, Colas J, Nguyen-Khoa T *et al.* (2010). Cystic fibrosis transmembrane regulator inhibitors CFTR(inh)-172 and GlyH-101 target mitochondrial functions, independently of chloride channel inhibition. J Pharmacol Exp Ther 333: 60–69.

l'Hoste S, Chargui A, Belfodil R, Corcelle E, Duranton C, Rubera I *et al.* (2010). CFTR mediates apoptotic volume decrease and cell death by controlling glutathione efflux and ROS production in cultured mice proximal tubules. Am J Physiol Renal Physiol 298: F435–F453.

L'Hoste S, Chargui A, Belfodil R, Duranton C, Rubera I, Mograbi B *et al.* (2009). CFTR mediates cadmium-induced apoptosis through modulation of ROS level in mouse proximal tubule cells. Free Radic Biol Med 46: 1017–1031.

Lu M, Ding C (2012). CFTR-mediated Cl(–) transport in the acinar and duct cells of rabbit lacrimal gland. Curr Eye Res 37: 671–677.

Ma T, Thiagarajah JR, Yang H, Sonawane ND, Folli C, Galietta LJ *et al.* (2002). Thiazolidinone CFTR inhibitor identified by high-throughput screening blocks cholera toxin-induced intestinal fluid secretion. J Clin Invest 110: 1651–1658.

Milosavljevic N, Duranton C, Djerbi N, Puech PH, Gounon P, Lagadic-Gossmann D *et al.* (2010). Nongenomic effects of cisplatin: acute inhibition of mechanosensitive transporters and channels without actin remodeling. Cancer Res 70: 7514–7522.

Muanprasat C, Sonawane ND, Salinas D, Taddei A, Galietta LJ, Verkman AS (2004). Discovery of glycine hydrazide pore-occluding CFTR inhibitors: mechanism, structure-activity analysis, and *in vivo* efficacy. J Gen Physiol 124: 125–137.

Muanprasat C, Wongborisuth C, Pathomthongtaweechai N, Satitsri S, Hongeng S (2013). Protection against oxidative stress in beta thalassemia/hemoglobin E erythrocytes by inhibitors of glutathione efflux transporters. PLoS ONE 8: e55685.

Peyronnet R, Sharif-Naeini R, Folgering JH, Arhatte M, Jodar M, El Boustany C *et al.* (2012). Mechanoprotection by polycystins against apoptosis is mediated through the opening of stretch-activated K(2P) channels. Cell Rep 1: 241–250.

Rich DP, Anderson MP, Gregory RJ, Cheng SH, Paul S, Jefferson DM *et al.* (1990). Expression of cystic fibrosis transmembrane conductance regulator corrects defective chloride channel regulation in cystic fibrosis airway epithelial cells. Nature 347: 358–363.

Rubera I, Duranton C, Melis N, Cougnon M, Mograbi B, Tauc M (2013). Role of CFTR in oxidative stress and suicidal death of renal cells during cisplatin-induced nephrotoxicity. Cell Death Dis 4: e817.

Sondo E, Tomati V, Caci E, Esposito AI, Pfeffer U, Pedemonte N *et al.* (2011). Rescue of the mutant CFTR chloride channel by pharmacological correctors and low temperature analyzed by gene expression profiling. Am J Physiol Cell Physiol 301: C872–C885.

Stahl M, Stahl K, Brubacher MB, Forrest JN Jr (2012). Divergent CFTR orthologs respond differently to the channel inhibitors CFTRinh-172, glibenclamide, and GlyH-101. Am J Physiol Cell Physiol 302: C67–C76.

Tabcharani JA, Low W, Elie D, Hanrahan JW (1990). Low-conductance chloride channel activated by cAMP in the epithelial cell line T84. FEBS Lett 270: 157–164.

Taddei A, Folli C, Zegarra-Moran O, Fanen P, Verkman AS, Galietta LJ (2004). Altered channel gating mechanism for CFTR inhibition by a high-affinity thiazolidinone blocker. FEBS Lett 558: 52–56.

Thiagarajah JR, Broadbent T, Hsieh E, Verkman AS (2004). Prevention of toxin-induced intestinal ion and fluid secretion by a small-molecule CFTR inhibitor. Gastroenterology 126: 511–519.

Vennekens R, Trouet D, Vankeerberghen A, Voets T, Cuppens H, Eggermont J *et al.* (1999). Inhibition of volume-regulated anion channels by expression of the cystic fibrosis transmembrane conductance regulator. J Physiol 515 (Pt 1): 75–85.

Wang L, Ma W, Zhu L, Ye D, Li Y, Liu S *et al.* (2012). ClC-3 is a candidate of the channel proteins mediating acid-activated chloride

currents in nasopharyngeal carcinoma cells. Am J Physiol Cell Physiol 303: C14–C23.

Wangemann P, Wittner M, Di Stefano A, Englert HC, Lang HJ, Schlatter E *et al*. (1986). Cl(–)-channel blockers in the thick ascending limb of the loop of Henle. Structure activity relationship. Pflugers Arch 407 (Suppl. 2): S128–S141.

Yang B, Sonawane ND, Zhao D, Somlo S, Verkman AS (2008). Small-molecule CFTR inhibitors slow cyst growth in polycystic kidney disease. J Am Soc Nephrol 19: 1300–1310.

Zhang WK, Wang D, Duan Y, Loy MM, Chan HC, Huang P (2010). Mechanosensitive gating of CFTR. Nat Cell Biol 12: 507–512.